JGR Space Physics

RESEARCH ARTICLE
10.1029/2018JA026259

This article is a companion to Zhao et al. (2019), https://doi.org/10.1029/2018JA026257.

Special Section:
Particle Dynamics in the Earth's Radiation Belts

Multiyear Measurements of Radiation Belt Electrons: Acceleration, Transport, and Loss

Daniel N. Baker[1], Vaughn Hoxie[1], Hong Zhao[1], Allison N. Jaynes[2], Shri Kanekal[3], Xinlin Li[1], and Scot Elkington[1]

[1]Laboratory for Atmospheric and Space Physics, University of Colorado, Boulder, CO, USA, [2]Physics and Astronomy, University of Iowa, Iowa City, IA, USA, [3]NASA/Goddard Space Flight Center, Greenbelt, MD, USA

Key Points:
- Essential factors are plentiful substorm "seed particles" and high-speed ($V > 500$ km/s) solar wind forcing
- The entire relativistic electron population can be wiped out in a few hours by shock wave impact but can rapidly be replenished
- Very long intervals have been observed without multimegaelectron volt electrons in the outer belt due to low solar wind driving

Correspondence to:
D. N. Baker,
daniel.baker@lasp.colorado.edu

Citation:
Baker, D. N., Hoxie, V., Zhao, H., Jaynes, A. N., Kanekal, S., Li, X., & Elkington, S. (2019). Multiyear measurements of radiation belt electrons: Acceleration, transport, and loss. *Journal of Geophysical Research: Space Physics*, *124*, 2588–2602. https://doi.org/10.1029/2018JA026259

Received 14 NOV 2018
Accepted 3 JAN 2019
Accepted article online 13 MAR 2019
Published online 10 APR 2019

Abstract In addition to clarifying morphological structures of the Earth's radiation belts, it has also been a major achievement of the Van Allen Probes mission to understand more thoroughly how highly relativistic and ultrarelativistic electrons are accelerated deep inside the radiation belts. Prior studies have demonstrated that electrons up to energies of 10 megaelectron volts (MeV) can be produced over broad regions of the outer Van Allen zone on timescales of minutes to a few hours. It often is seen that geomagnetic activity driven by strong solar storms (i.e., coronal mass ejections, or CMEs) almost inexorably leads to relativistic electron production through the intermediary step of intense magnetospheric substorms. In this study, we report observations over the 6-year period 1 September 2012 to 1 September 2018. We focus on data about the relativistic and ultrarelativistic electrons ($E \geq 5$ MeV) measured by the Relativistic Electron-Proton Telescope sensors on board the Van Allen Probes spacecraft. This work portrays the radiation belt acceleration, transport, and loss characteristics over a wide range of geomagnetic events. We emphasize features seen repeatedly in the data (three-belt structures, "impenetrable" barrier properties, and radial diffusion signatures) in the context of acceleration and loss mechanisms. We especially highlight solar wind forcing of the ultrarelativistic electron populations and extended periods when such electrons were absent. The analysis includes new display tools showing spatial features of the mission-long time variability of the outer Van Allen belt emphasizing the remarkable dynamics of the system.

1. Introduction

A principal goal of the Radiation Belt Storm Probes (RBSP) mission was to develop a much deeper understanding of the structure and time variability of Earth's radiation belts. Almost immediately after the late-August 2012 launch of the dual RBSP spacecraft into their highly elliptical orbits, it was discovered that a third Van Allen belt (or "storage ring") of highly relativistic electrons can exist near the inner part of the traditionally recognized outer Van Allen zone (Baker et al., 2013). This feature has been the subject of much theoretical investigation and speculation since its discovery.

In addition to morphological structures of the radiation zones such as the third belt, it has also been a major achievement of the RBSP program (renamed the "Van Allen Probes" mission in November 2012) to understand more thoroughly how ultrarelativistic electrons are accelerated deep inside the radiation belts due to various wave-particle interactions (e.g., Thorne et al., 2013). Van Allen Probes studies have demonstrated that electrons up to energies of order 10 megaelectron volts (MeV) can be produced over broad regions of the outer Van Allen zone on surprisingly short timescales (Foster et al., 2014, 2015). The key to such rapid acceleration is the interaction of "seed" populations of ~30- to ~300-keV electrons with electromagnetic waves in the lower band whistler-mode chorus frequency range (e.g., Jaynes et al., 2015). On somewhat longer timescales ultralow frequency (ULF) waves can play a strong role in driving radial diffusion as well (Li et al., 2009; Mann et al., 2016; Zhao et al., 2018a; Jaynes et al., 2018).

Extended studies of Van Allen Probes data show that "source" electrons (in a typical energy range of one to a few tens of kiloelectron volts) produced by magnetospheric substorms play a crucial role in amplifying the chorus waves in the magnetosphere. It is very often observed that these chorus waves then rapidly heat and accelerate the tens to hundreds of kiloelectron volts seed electrons that are injected by substorms into the outer Van Allen zone. Thus, geomagnetic activity driven by strong solar storms (coronal mass ejections or CMEs) regularly leads to ultrarelativistic electron production through the intermediary step of intense

magnetospheric substorms (Jaynes et al., 2015). When substorms are weak or absent, radiation belt enhancements are not able to occur.

In this paper, we report long-term radiation belt observations and also focus individually on the largest geomagnetic storms of the last several years. Distinctive events that exhibited significant ring current development are discussed. We focus on storms that produced large effects on the relativistic and ultrarelativistic electrons measured by the Relativistic Electron-Proton Telescope (REPT) sensors (Baker et al., 2012) on board the Van Allen Probes spacecraft. This paper describes the radiation belt acceleration, transport, and loss characteristics for these intense geomagnetic events. We emphasize features seen repeatedly in the data (three-belt structures, "impenetrable" barrier properties, and radial diffusion signatures) in the context of acceleration and loss mechanisms. We especially highlight solar wind forcing of the ultrarelativistic ($E \geq 5$ MeV) electron populations. We address energy-spectral issues for key events. We also focus on special periods of many months duration where highly relativistic electrons were entirely absent throughout the entire outer Van Allen zone. The presentation includes new visualization tools portraying the time variability of the outer Van Allen belt emphasizing the remarkable dynamics of the system.

2. Data Sets

A primary data set for this study consists of the energetic particle measurements made using the REPT instrument on board the dual-spacecraft Van Allen Probes mission. Baker et al. (2012) described in detail the REPT design and measurement capabilities. While the REPT instruments also make comprehensive measurements of energetic protons across a wide energy span ($E \sim 15$ MeV to $E > 400$ MeV) throughout the radial range of the Van Allen Probes (see Selesnick, 2015; Selesnick et al., 2018), the principal focus in the present study is upon relativistic electron fluxes from $E \sim 1.5$ MeV to $E \geq 10$ MeV. Several prior studies have examined limited time intervals of REPT electron data (Baker et al., 2013, 2015, 2016; Baker, Jaynes, Li, et al., 2014; Kanekal et al., 2015), but the present work looks at the complete set of REPT measurements for the period 1 September 2012 to 1 September 2018. In general, the REPT data from the RBSP-A and RBSP-B spacecraft are cross-calibrated to within 1% of one another. Thus, we are able to combine the REPT-A and REPT-B data seamlessly for our long-term studies presented here.

To support our radiation belt particle observations and to provide context for those measurements, we also utilize solar wind and interplanetary magnetic field (IMF) data from the "CDAWeb" data set (https://cdaweb.sci.gsfc.nasa.gov/). We typically use solar wind data averaged to daily values but also use multiple-day smoothing of the data in some analyses (as noted in the observation sections below).

3. Long-Term Radiation Belt Overview

Figure 1 provides a broad summary of radiation belt electron fluxes and concurrent solar wind and IMF data for the inclusive period 1 September 2012 to 1 September 2018. The top four panels show color-coded differential fluxes of energetic electrons as a function of L value (vertical axis) versus time (horizontal axis). For the purposes of this survey plot, the dipole L value is used to organize the data. The flux scale for each energy range is shown by the logarithmic color bar to the right side of each panel. The energy channels displayed are (a) 1.8 MeV, (b) 2.6 MeV, (c) 4.2 MeV, and (d) 6.3 MeV.

The lower four panels of Figure 1 show solar wind and IMF data for the same 6-year period of 2012–2018. Panel (e) shows 3-day running averages of the solar wind speed (V). Panel (f) shows the similarly averaged IMF B strength. Panel (g) shows the corresponding IMF B_z component for the entire interval, and panel (h) shows the interplanetary y component of the solar wind electric field ($-E_y \sim VB_z$).

Several features can be noted about the relativistic electron behavior in Figure 1. While comparatively high fluxes often were seen (especially in the lower energy channels) during late 2012 and into 2013, during most of 2014 the electron fluxes were quite low. In fact, for the 4.2- and 6.3-MeV energy channels there were virtually no measurable fluxes for the entire year of 2014. In contrast, in 2015 and subsequent years (up to ~December 2017) the electron fluxes were often quite high. Looking at the solar wind speed data (panel e), it is obvious that V_{sw} values were continuously low in 2014, essentially never exceeding 500 km/s during that entire year. On the other hand, for the period 2015–2017, the solar wind speed was

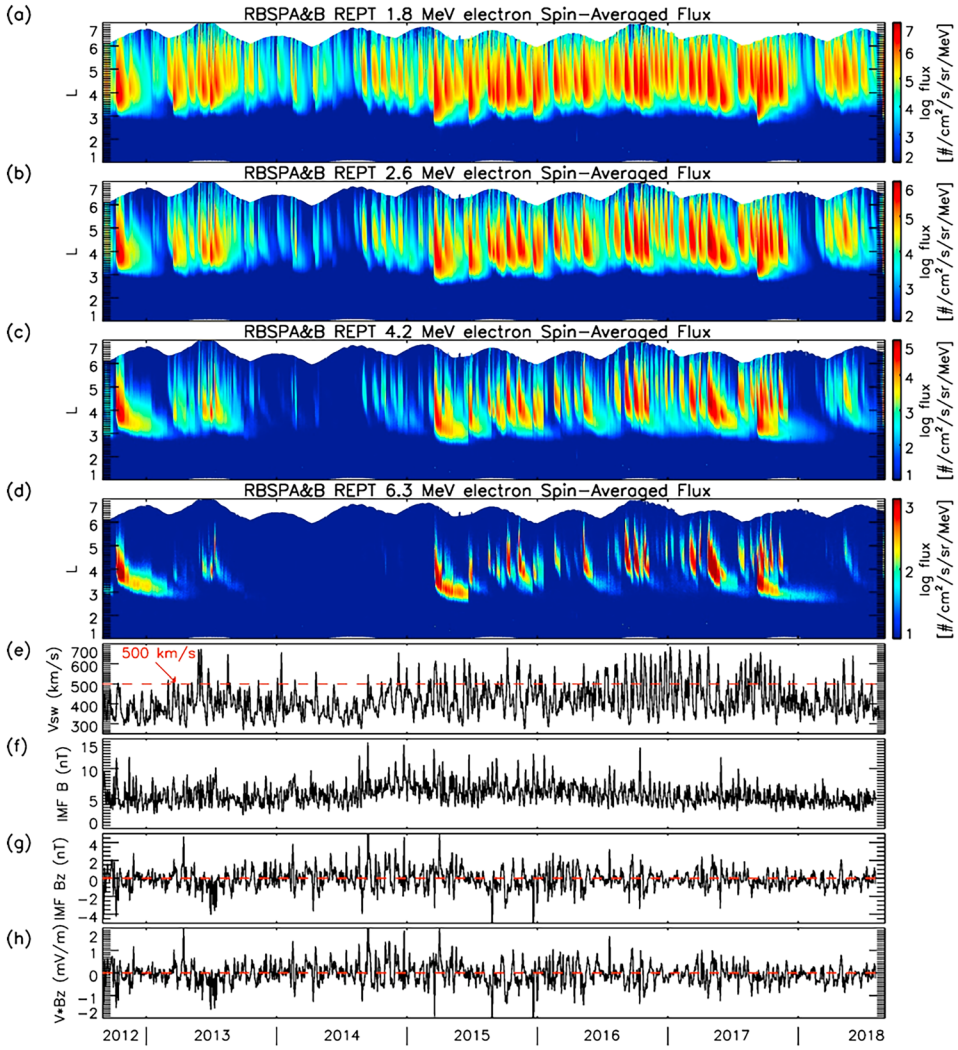

Figure 1. (a–d) Spin-averaged fluxes of electrons with energies of 1.8, 2.6, 4.2, and 6.3 MeV from 1 September 2012 to 1 September 2018, using data from both Van Allen Probes. (e–h) Three-day running averaged solar wind speed, IMF B, IMF B_Z, and VB_Z during the same time period. RBSP = Radiation Belt Storm Probes; REPT = Relativistic Electron-Proton Telescope.

frequently above 500 km/s and, furthermore, often showed clear periodic behavior characteristics of recurrent high-speed solar wind streams (e.g., McPherron et al., 2009). Such streams are known to set up efficient accelerator conditions for high-energy electrons (Baker et al., 1997; Li et al., 2011; McPherron et al., 2009). We note that for late 2017 and the early portion of 2018, the radiation belts again showed a paucity of particles for a quite extended interval rather similar to that seen in 2014.

There were several particularly strong and distinctive electron acceleration events evident in the long-term REPT data of Figure 1. One of those in October 2012 has been much studied (Reeves et al., 2013) and was due to an effective CME structure hitting the magnetosphere commencing on 8 October 2012. Powerful acceleration was observed across all Van Allen Probes electron energy channels and clearly extended up to at least 6.3 MeV (see Figure 1d). Another clear, CME-driven relativistic electron event occurred on 17 March of 2013 (see Baker, Jaynes, Li, et al., 2014; Foster et al., 2014). This event was abrupt and powerful but did not register as strongly in the $E = 6.3$-MeV channel as did the October 2012 storm.

The largest electron acceleration event of the Van Allen Probes era occurred on 17 March 2015. This event has been studied in detail by Baker et al. (2016). In their analysis, Baker et al. showed that the March 2015 CME impact completely depleted the outer radiation belt and then subsequently allowed rapid

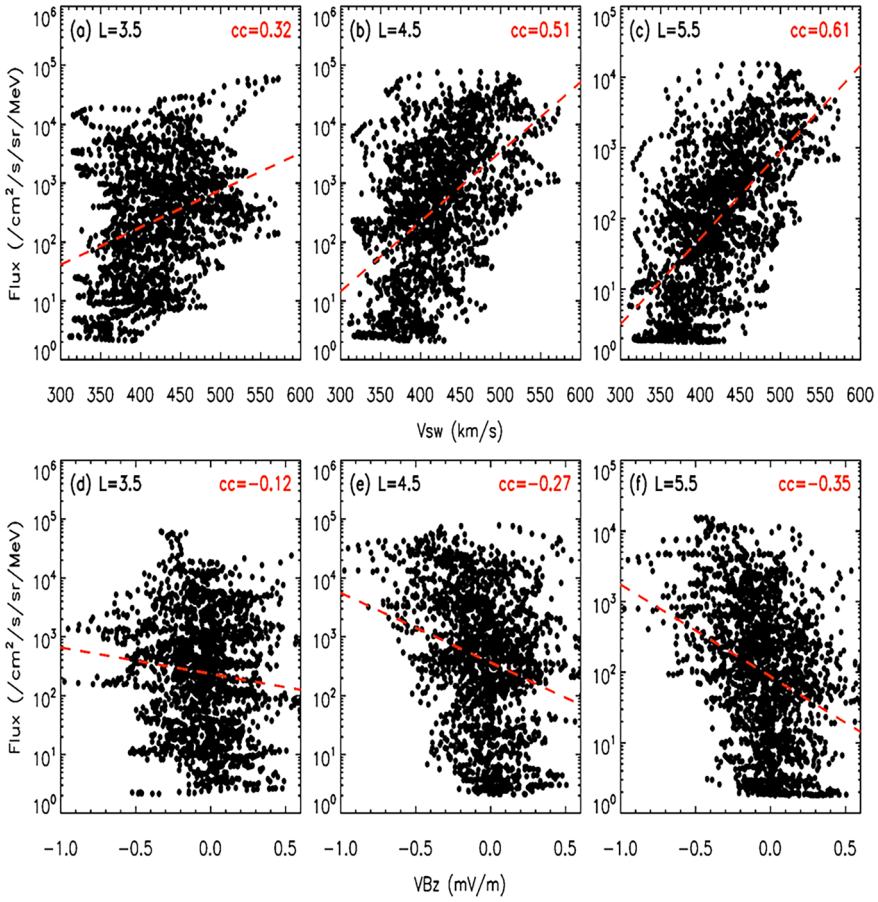

Figure 2. Scatterplots of 13-day running averaged 4.2-MeV electron fluxes and 13-day running averaged (top) solar wind speed and (bottom) VB_z, using data from both Van Allen Probes from 1 September 2012 to 1 September 2018.

reacceleration of electrons up to at least 8–10 MeV. A subsequent geomagnetic storm in June 2015 also produced powerful radiation belt effects, in several ways building rapidly upon the remnants of the March 2015 storm.

A fourth storm quite worthy of detailed analysis occurred in September 2017. Note in Figure 1 that this storm was similarly powerful in radiation belt response to the March 2015 period. Electrons in energy from $E \sim 1$ MeV all the way up to 10 MeV (or greater) were suddenly produced across all outer belt L-shells on 7 and 8 September 2017 (as will be shown below). Like the October 2012 storm and the March 2015 storm, the September 2017 storm produced a long-lasting and slowly decaying electron population seen, for example, in the $E \sim 6.3$-MeV energy channel near $L \sim 3.0$.

A feature seen in the data of Figure 1 is that at no time, and at none of the plotted energies, did a detectable flux of electrons penetrate directly, or get accelerated within, the region $L \leq 2.8$. This seeming "impenetrable" barrier to relativistic electron inward motion was reported in Baker, Jaynes, Hoxie, et al. (2014). This barrier and its relationship to VLF wave fields also measured by Van Allen Probes have been discussed in detail by Foster et al. (2016).

4. Statistical Relationships

As becomes clear from careful examination of Figures 1e–1h, there are several broad correlations between electron flux levels (Figures 1a–1d) and key solar wind and IMF parameters. We have already pointed out, for example, that peak solar wind speeds were commonly above 500 km/s in 2015–2017 but were lower during 2014. We also note some tendency for the IMF B_z component to be more strongly and frequently negative (southward) during 2015–2016 than (say) for much of 2014. However, visual inspection of

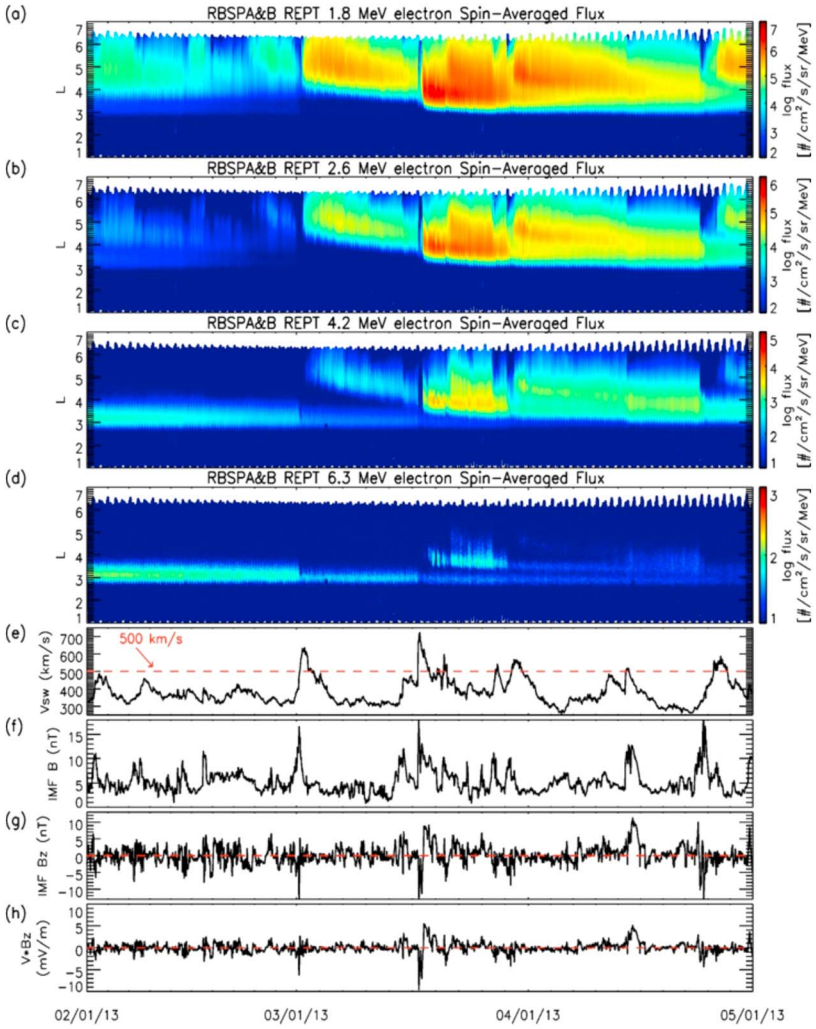

Figure 3. (a–d) Spin-averaged fluxes of electrons with energies of 1.8, 2.6, 4.2, and 6.3 MeV from 1 February to 1 May 2013, using data from both Van Allen Probes. (e–h) One-hour solar wind speed, IMF B, IMF B_Z, and VB_Z during the same period. RBSP = Radiation Belt Storm Probes; REPT = Relativistic Electron-Proton Telescope.

relationships from plots such as Figure 1 cannot be completely convincing or quantitative concerning correlation strengths.

In order to examine energetic electron flux relationships more deliberately with solar wind conditions, we have carried out a wide range of statistical comparisons (only a small portion of which are explicitly presented here). For these purposes, we have taken flux "cuts" at several fixed L values (L = 3.5, 4.5, and 5.5) for each of the REPT electron energy channels. This gives a basic daily average value for the flux at the several energies, which we have then compared with corresponding solar wind and IMF parameters. We initially compared single-day V_{sw} and IMF values with electron fluxes. These were interesting but were rather highly scattered. Since relativistic electron fluxes in the outer zone tend to persist for many days after being first accelerated, we opted to use more highly smoothed solar wind and IMF parameters for our statistical comparisons. Here we choose to show scatter plots of daily increments but with V_{sw} and IMF values smoothed by a running 13-day filter. Such a filter tends to reduce IMF fluctuations and takes cognizance of the kind of high-speed solar wind stream driving common in 2016–2017 (see above). Figure 2 shows such scatter plots for electrons with E = 4.2 MeV for the entire 6-year run of data. Panel (a) is the cut of fluxes at L = 3.5 (see Figure 1c) versus the concurrent values of solar wind speed. Similarly, panel (b) is for E = 4.2-MeV fluxes at L = 4.5 versus V, and panel (c) is for E = 4.2-MeV fluxes at L = 5.5 versus V. The lower row in Figure 2 is for 4.2-MeV fluxes versus the parameter VB_z for L = 3.5, 4.5, and 5.5.

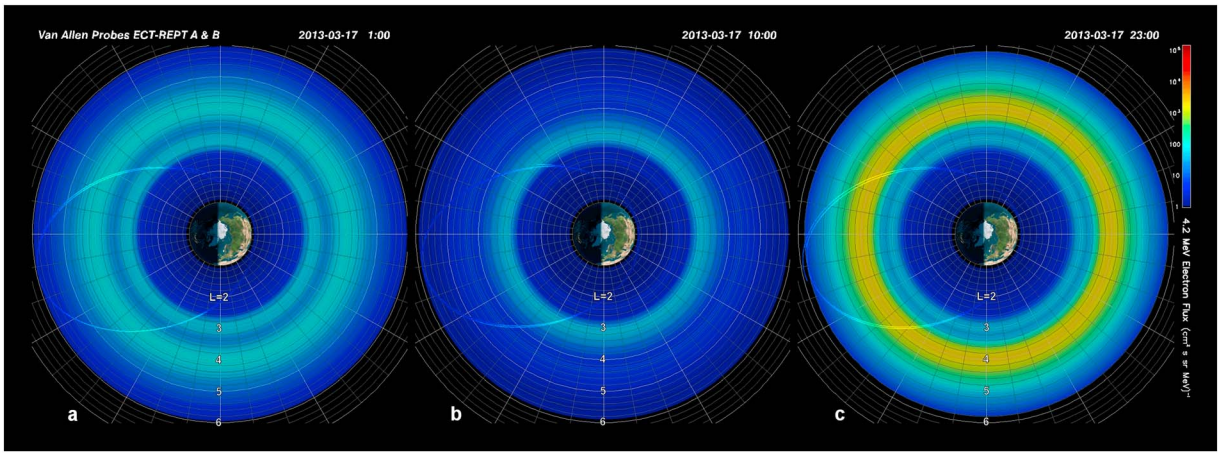

Figure 4. Polar plots for 4.2-MeV channel for 17 March 2013. (a) Pattern for ~0100UT. (b) For ~1000UT. (c) For ~2300UT for times shown. ECT = Energetic particle, Composition, and Thermal plasma; REPT = Relativistic Electron-Proton Telescope.

In general, we see that 4.2-MeV electron fluxes correlate positively with V_{sw} at all L values but that the correlations become considerably stronger at higher L values. This kind of flux relationship with solar wind speed was noted earlier (e.g., Baker et al., 1997; Baker, Kanekal, & Blake, 2004; Reeves et al., 2011; Zhao et al., 2017). On the other hand, the correlations of electron flux with VB_z (Figures 2d–2f) were found to be considerably weaker than for V_{sw} alone. Thus, in keeping with several prior studies, we find V_{sw} to be a dominant controller of relativistic electron increases—especially in the outermost part of the outer Van Allen zone. The trends found for E ~ 4.2 MeV in Figure 2 were generally similar for both lower and higher energies measured by REPT during 2012–2018. Obviously, from results shown here, we conclude that correlation strengths were not extremely high for any solar wind drivers. For the largest correlation coefficients (i.e., r ~ 0.6) only about 40% (r^2) of the variance of flux changes can be explained by solar wind drivers. Thus, other (internal) magnetospheric processes must play a large role in flux variability.

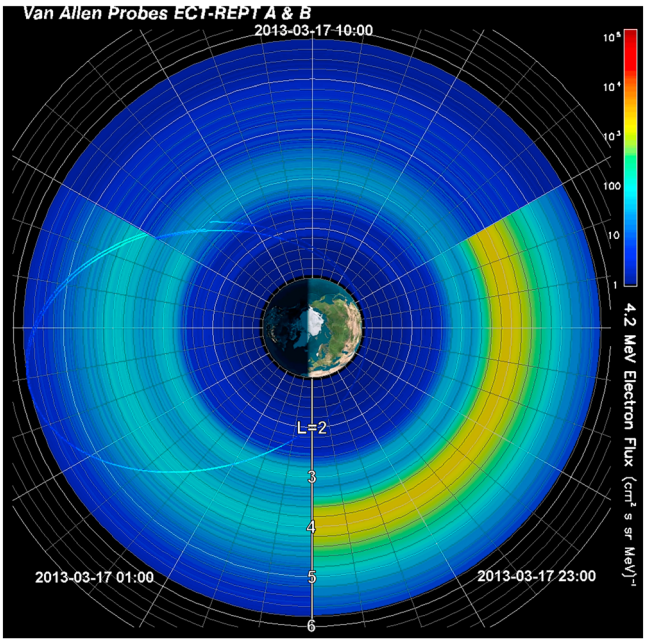

Figure 5. Merged polar plots for 4.2-MeV channel for 17 March 2013 comparing the several periods shown in Figure 4. ECT = Energetic particle, Composition, and Thermal plasm; REPT = Relativistic Electron-Proton Telescope.

5. Strongest Solar Wind Forcing Intervals

Several of the strongest relativistic electron depletion intervals that were rapidly followed by strong electron flux enhancements deserve special attention here. As a consequence, we examine March 2013, March 2015, and September 2017 closely in this section using our latest display tools. We recall for reference that March 2013 and March 2015 were analyzed previously in some detail by our team (Baker et al., 2016; Baker, Jaynes, Li, et al., 2014; Foster et al., 2014).

5.1. March 2013 Period

Figure 3 shows a blown-up time segment of the same data and solar wind parameters that initially were shown in Figure 1. The interval portrayed in Figure 3 is 1 February 2013 to 1 May 2013. This broad period of time fully envelops the strong CME interaction and shock wave impact that occurred on 17 March 2013. It is readily seen from Figure 3 that the solar wind speed went to high values (>600 km/s) around the time of the shock wave passage and the IMF was strongly southward for a long period of time during the CME passage.

Figure 3 makes the strikingly obvious point that essentially whenever the solar wind speed goes substantially above 500 km/s for an extended period of time, the result is the initiation of a relativistic electron flux enhancement. While this is not a new observation (see, for example, Baker et al., 1997), nonetheless, the Van Allen Probes data show this effect with stark

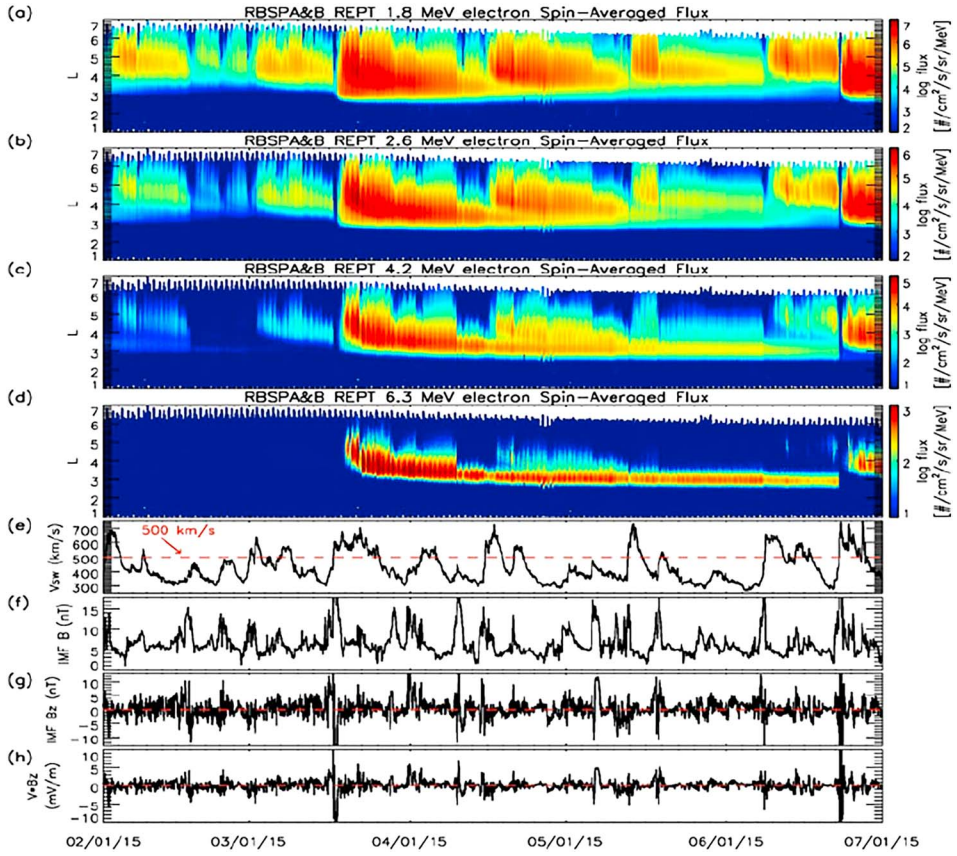

Figure 6. Similar format to Figure 3 but for the time period of 1 February to 1 July 2015. RBSP = Radiation Belt Storm Probes; REPT = Relativistic Electron-Proton Telescope.

clarity. The electron flux onset around 1 March 2013 was a solar wind stream-driven enhancement (Baker, Jaynes, Li, et al., 2014), while the 17 and 30 March events were CME-driven examples. This was also the case for the event that occurred on ~20 April 2013 (toward the right side of Figure 3).

Figure 4 is a new visualization tool for looking at daily "maps" of radiation belt fluxes derived from fluxes of electrons sampled along the RBSP spacecraft orbits. The image in each panel of Figure 4 shows a view looking down from above the North Pole onto the magnetic equatorial plane. The sun is to the right in each image and the orbital traces for the Van Allen Probes A and B spacecraft are shown for the times indicated

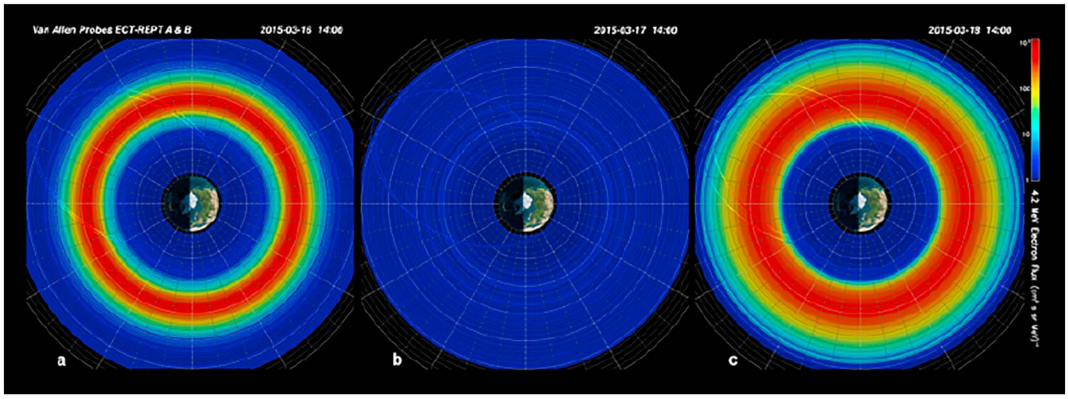

Figure 7. Similar to Figure 4 for 16–18 March 2015. ECT = Energetic particle, Composition, and Thermal plasm; REPT = Relativistic Electron-Proton Telescope.

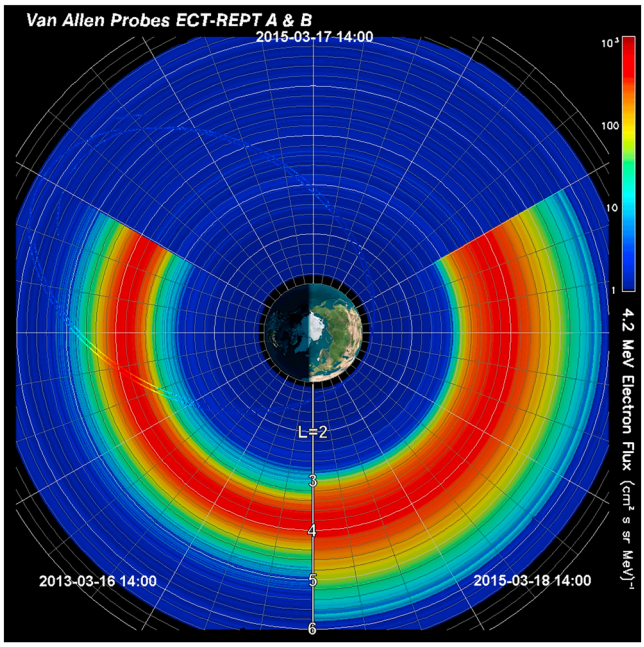

Figure 8. Similar to Figure 5 for 16 and 17 March 2015. ECT = Energetic particle, Composition, and Thermal plasm; REPT = Relativistic Electron-Proton Telescope.

in each panel. The absolute intensity of the differential particle flux at $E \sim 4.2$ MeV is shown along the trajectory profile according to the logarithmic color bar to the right of the figure.

We recognize that on timescales (minutes to tens of minutes) that are short compared to the 9-hr orbital period of the Van Allen Probes, the measured 4.2-MeV electrons will drift completely around the Earth due to magnetic gradient and curvature drift effects. Thus, we can—with reasonable accuracy—map the fluxes measured along the spacecraft pathway all the way around the Earth on dipole L-shells. The images in Figures 4a–4c represent such an azimuthal pattern due to magnetic gradient and curvature mapping of the measurements made by the REPT A and B sensors.

In Figure 4a, we see the pattern of electron flux levels for the period on 17 March 2013 at about 0100 UT, that is, just a short while before the interplanetary shock wave impacted the magnetosphere. We see a very clear illustration of the double-ring outer belt structure (Baker et al., 2013) in this figure. The inner (storage ring) feature was quite distinct and separated from the rest of the outer belt of highly relativistic electrons in this case.

Figure 4b shows the comparable REPT data at 1000UT on 17 March just a few hours after the shock passage time (0645UT) on this day. In this frame, we see that the outer ring of $E \sim 4.2$-MeV electrons was swept away leaving only the storage ring population. Given the completeness and speed of the outer belt electron removal, one gets a sense of how efficient and rapid electron loss can be during CME impact events. Figure 4c shows REPT A and B data just one orbital period later at 2300UT on 17 March 2013. At this time, the multi-MeV electrons throughout the outer zone had largely been restored (see Foster et al., 2014; and Baker, Jaynes, Li, et al., 2014 for details.) Note that the "third" belt or storage ring around $L = 3.0$ remained intact throughout this whole period.

Figure 5 arrays together segments of the polar-projected data in Figure 4 from the three time periods on 17 March 2013 in one single plot. In this way, it shows in a clear fashion that outer zone electrons can be lost in a comparative instant when a shock wave strikes the system. The storage ring feature may appear (in magnetic dipolar L coordinates, at least) to be somewhat distorted after shock passage. But then, as the system recovered, high-energy electrons were—in a matter of hours—fully reenergized and distributed throughout the outer belt, while the third belt was persistently maintained.

5.2. March 2015 Period

Figure 6 is analogous to Figure 3 but shows data for the period 1 February to 1 July 2015. This period encompassed demonstrably the strongest geomagnetic storm of solar cycle 24 (and this commenced on 17 March 2015). There was another strong geomagnetic storm in June 2015. Both the March and June events were driven by powerful CME impacts (see Baker et al., 2016). The inward radial motion of the ultrarelativistic electrons was of deeper extent ($L \sim 2.6$) during the March 2015 event than during any other period during the Van Allen Probes era.

The interplanetary shock wave ahead of the CME responsible for the 17 March 2015 geomagnetic storm struck the Earth's magnetosphere at 0445UT on 17 March (see Baker et al., 2016). This initiated a sharp storm sudden commencement and also set in motion a strong depletion of the entire outer radiation belt across all REPT-measured energies. As discussed in Baker et al. (2016), the swiftness and completeness of the outer belt depletion on 17 March was remarkable. By early on 18 March 2015, however, the radiation belt electrons up to multiple-MeV energies were quite fully restored and reached flux levels much higher than prior to the shock arrival. Another interesting feature of this event was the prompt energization of electrons at ultrarelativistic energies within <2 min of the shock passage, which injected electrons deep into the magnetosphere ($L < \sim 3$; Kanekal et al., 2016).

Figure 7 is analogous to Figure 4 above and shows polar perspectives of $E = 4.2$-MeV electron fluxes for 16–18 March 2015. In Figure 7a, we present azimuthally mapped flux profiles for ~1400UT on 16 March.

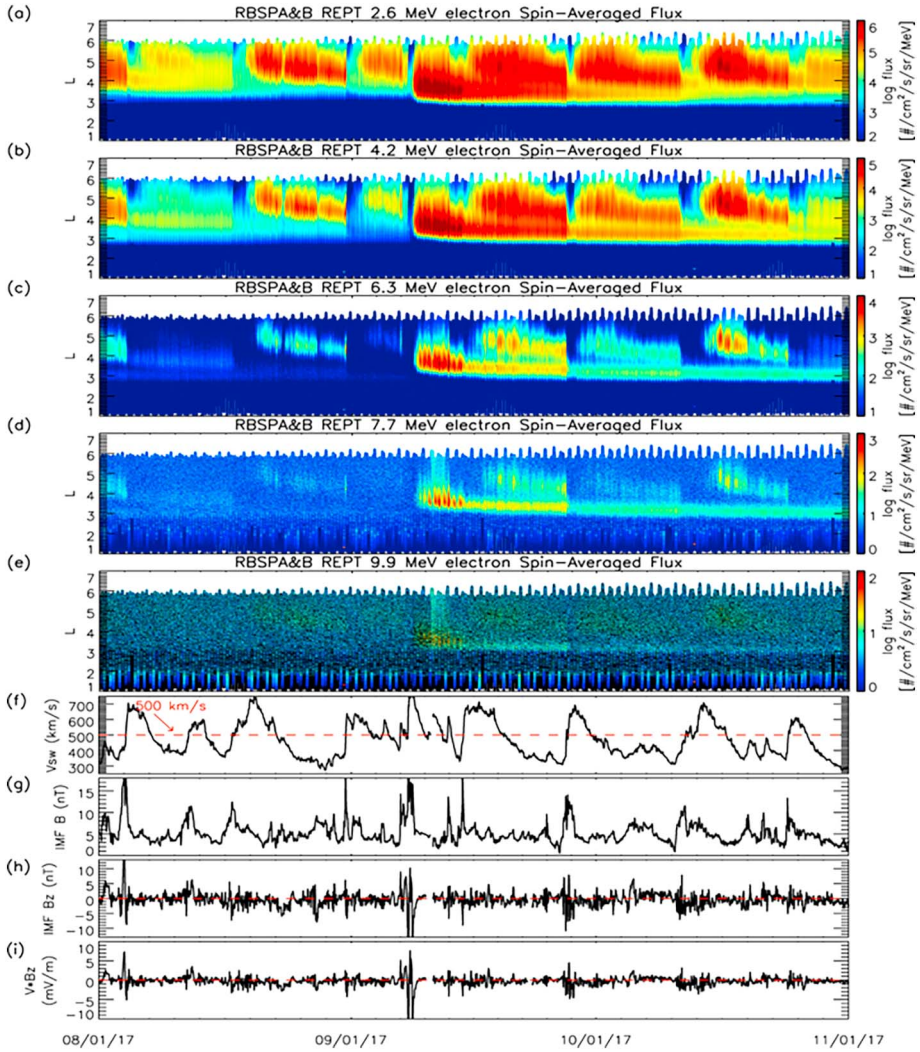

Figure 9. (a–e) Spin-averaged fluxes of electrons with energies of 2.6, 4.2, 6.3, 7.7, and 9.9 MeV from 1 August to 1 November 2017, using data from both Van Allen Probes. (f–i) One-hour solar wind speed, IMF B, IMF B_z, and VB_z during the same time period. RBSP = Radiation Belt Storm Probes; REPT = Relativistic Electron-Proton Telescope.

There was a relatively intense outer belt population extending from $L \sim 2.9$ (the typical outward edge of the "barrier") out to $L \simeq 4.2$. As shown in Baker et al. (2016), this outer belt configuration had been set up over a period of nearly 3 weeks by gradual inward radial diffusion following a high-speed solar wind stream that struck the magnetosphere in early March 2015.

Figure 7b shows REPT measurements at $E = 4.2$ MeV for the period around 1400UT on 17 March, that is, about 10 hr following the shock wave impact. As is clear from the figure, there were essentially no measurable fluxes of multi-MeV electrons detectable at any radial location in this postshock impact interval. However, as is clear from Figure 7c, by 1400UT on 18 March, the outer belt population was fully and quite substantially replenished. In fact, the inner edge of the outer belt was pushed into $L \sim 2.8$ and high fluxes extended well outward beyond $L \sim 5.5$.

In analogy with Figure 5 above, Figure 8 shows a composite diagram made up of segments from Figures 7a–7c. This illustrates the remarkable and dynamic variability of the outer belt electron population during strong CME-driven events. As also shown above for the March 2013 case, in a period of order 1 day the radiation belts can go from a fairly placid, quiescent state to be essentially completely drained by rapid loss processes (see Shprits et al., 2015; Xiang et al., 2017). Subsequently, the outer belt can essentially be fully reconstituted on time scales of just hours.

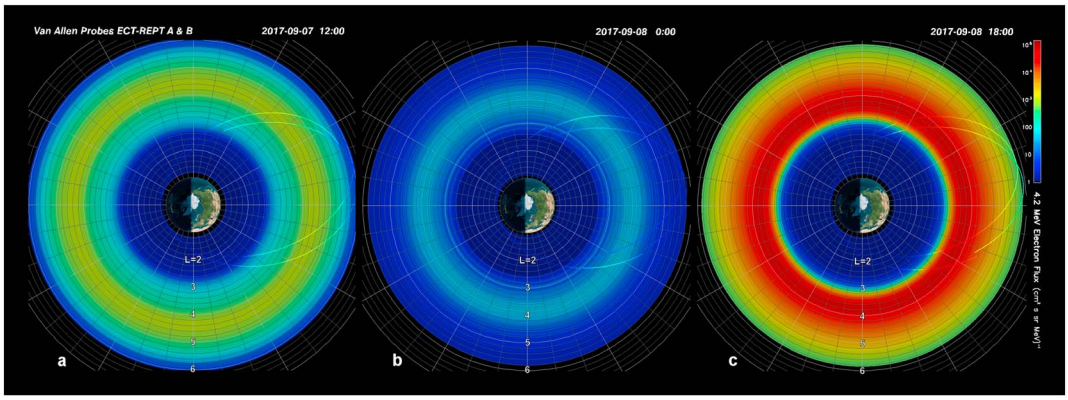

Figure 10. Similar to Figure 4 for 7 and 8 September 2017. ECT = Energetic particle, Composition, and Thermal plasm; REPT = Relativistic Electron-Proton Telescope.

5.3. September 2017 Period

Figure 9 is analogous to Figures 3 and 6 above. It provides an expanded view of REPT electron fluxes and solar wind conditions for the period 1 August to 1 November 2017. This period encompasses several high speed solar wind stream intervals and also contained an extremely strong CME-driven event (7 and 8 September) that produced wide-ranging outer radiation belt responses. As shown in Figure 9, in fact, this event demonstrates the clearest evidence of any Van Allen Probes era geomagnetic storm interval for direct electron acceleration to energies above 10 MeV. In Figure 9e, it seems clear that by 11 September, this storm had produced measurable fluxes of electrons lasting several days in the $E = 9.9$ MeV ($9.1 \leq E \leq 12.6$ MeV) REPT channel. Clearly in the $E = 7.7$-MeV channel (Figure 9d), the electrons produced by this storm formed the very high-energy storage ring (third belt) population that persisted until at least 1 November 2017. (In fact, examining Figure 1, this third belt lasted until well into 2018).

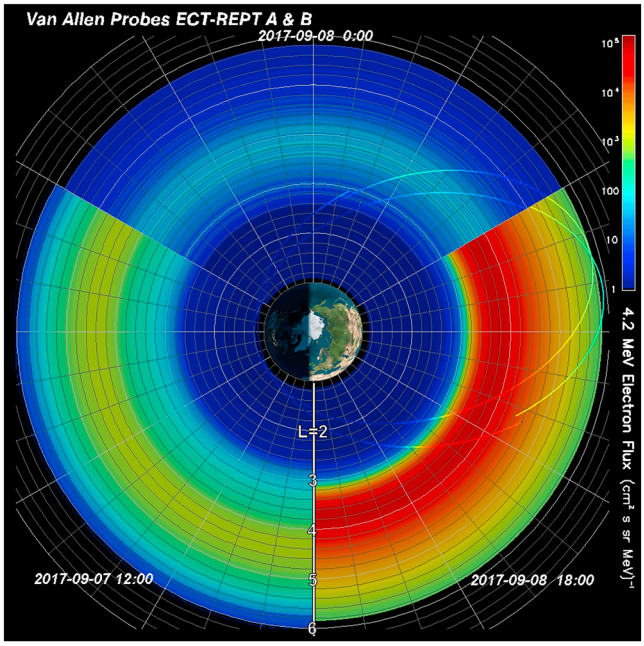

Figure 11. Similar to Figure 5 for 7 and 8 September 2017. ECT = Energetic particle, Composition, and Thermal plasm; REPT = Relativistic Electron-Proton Telescope.

Figure 9 shows a rich variety of electron acceleration, transport, and loss features during this August–October period. Numerous radial diffusion events were evident (as in late-August and in the period 17–27 September). These kinds of event are often superimposed upon the remnants of earlier acceleration events. At times (as on 31 August and again early on 7 September), there were fascinating brief bursts of accelerated electrons that were very transient. As rapidly as they appeared, they quickly disappeared. Each of these was associated with strong solar wind impulses (see Figures 9f–9i).

The central focus of Figure 9 is the events on 7 and 8 September 2017. The abrupt losses (related to an interplanetary shock impact) and the strong replenishment of the belts on 8 September are quite clear across a wide energy range. Figure 10 is analogous to Figures 4 and 7 above and shows polar projection maps of the radiation belt fluxes for the REPT $E = 4.2$-MeV channel. Figure 10a shows data for the period around 1200UT on 7 September. It is seen that the outer belt was very broad in radial extent ($2.8 \leq L \leq 5.8$) during that time. Peak electron intensities were relatively high across this entire range of geocentric distances. Figure 10b shows that by 0000UT on 8 September, most of the outer belt had been scoured away leaving only a rather complex storage ring population (from $L \sim 3.5$ to $L \sim 4.2$). Then, by 1800UT on 8 September, the outer zone was strongly repopulated by multi-MeV electrons extending (Figure 10c) from $L \sim 2.9$ out at least to $L \sim 4.6$.

Figure 11 is analogous to Figures 5 and 8 above. It shows by superposition of pieces of Figures 10a–10c that the outer zone was extraordinarily time

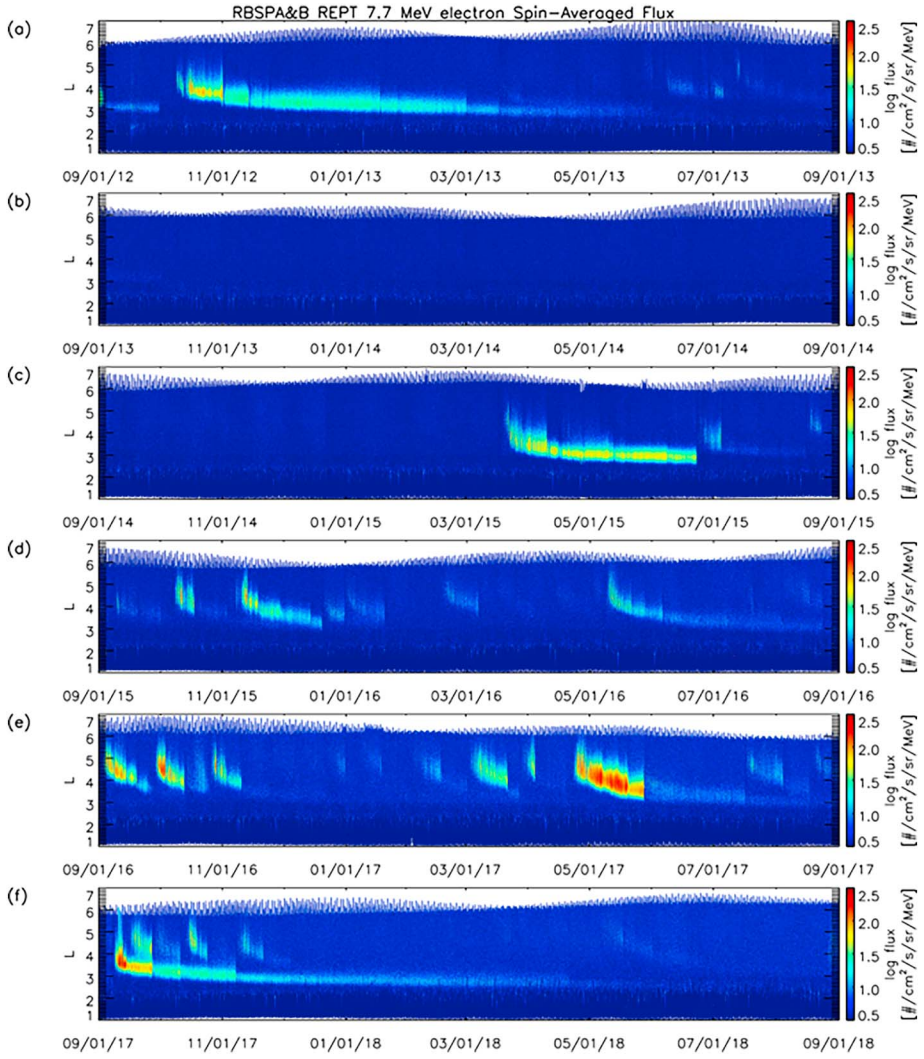

Figure 12. Spin-averaged 7.7-MeV electron fluxes shown year-by-year from 1 September 2012 to 1 September 2018. RBSP = Radiation Belt Storm Probes; REPT = Relativistic Electron-Proton Telescope.

variable during this forcing interval. In its regeneration after 8 September, the outer belt was much narrower in radial extent but much higher in average intensity.

6. Sporadic, Very High-Energy Events

The REPT instruments on board the two Van Allen Probes spacecraft have provided capabilities to measure higher-energy electrons than has been readily possible on prior magnetospheric missions. The combination of sensitivity, energy resolution, and background rejection have allowed the REPT sensors to systematically assess the occurrence and time dependence of electrons in the energy range of 7~12 MeV throughout the entire inner magnetosphere.

To illustrate this capability, in Figure 12, we show *L*-versus-time plots of the REPT channel labeled "$E = 7.7$ MeV." This is a differential channel that covers roughly 7- to 9-MeV electron energies. The figure shows six panels, each panel covering one full year of REPT measurements (commencing on 1 September of each year from 2012 to 2017). As can be seen from the plot, enhancement episodes at such high energies were relatively rare, especially in the period from September 2012 through early 2015. Only the October 2012 storm event during this time interval produced a long-lasting 7.7-MeV electron population. Similarly, the March 2015 storm (Figure 12c) showed a powerful high-energy enhancement that lasted prominently until

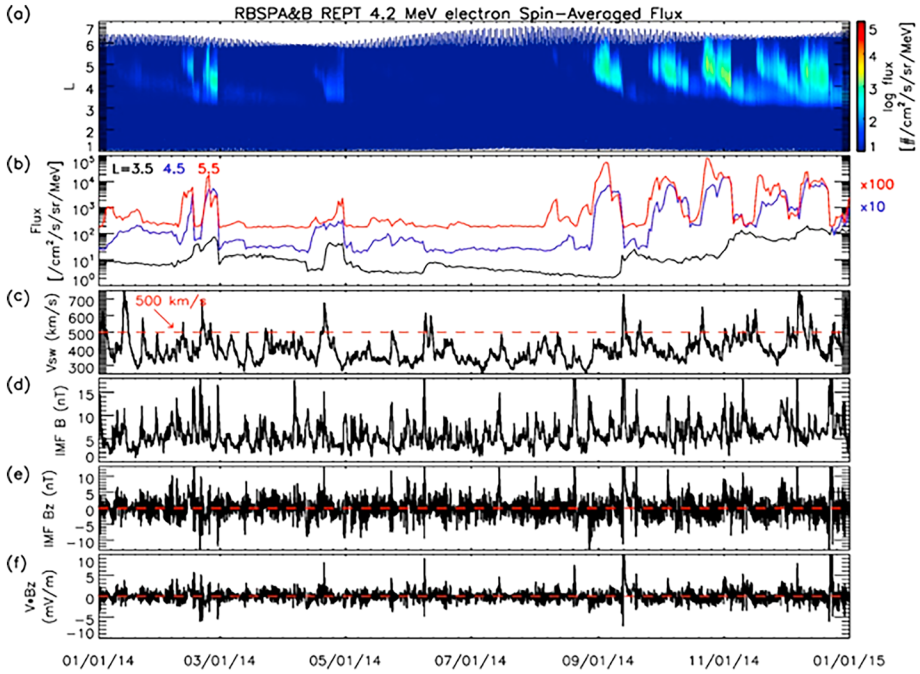

Figure 13. (a) Spin-averaged 4.2-MeV electron fluxes, (b) daily-averaged 4.2-MeV electron fluxes at $L = 3.5$, 4.5, and 5.5 (with fluxes at $L = 4.5$ multiplied by 10 and at $L = 5.5$ multiplied by 100), (c–f) One-hour solar wind speed, IMF B, IMF B_z, and VB_z, during 1 January 2014 to 1 January 2015. RBSP = Radiation Belt Storm Probes; REPT = Relativistic Electron-Proton Telescope.

the electrons were wiped out by the impact of the 22 June 2015 CME shock wave. This shock impact rapidly and completely depleted the entire outer zone population.

The later periods in 2015 through 2018 have shown numerous enhancements of $E \geq 7$-MeV electrons (Figures 12d–12f).

These all show a pattern of strong initial onset at relatively higher L-shell onset. Then the electron population appears to radially diffuse inward toward Earth until the inner edge of the flux enhancement reached $L \sim 2.8$. The population then remained in place and often gradually dissipated. But just as often, the population was dramatically lost (in a virtual instant) when a strong solar wind impulse or CME strikes the magnetosphere.

7. Extended Intervals of Electron Paucity

At the lowest energies measured by the REPT sensors, there was seldom a time during the 6-year period under scrutiny that did not show at least some measurable electron flux (See Figure 1). However, as one examines energies above 2–3 MeV, there were periods (as previously remarked) that had essentially no detectable electron fluxes anywhere in the magnetosphere. These times of great paucity of multi-MeV electrons deserve attention and understanding. In sections above, we focused on enhancement intervals; we can also learn a good deal about the system behavior by studying times completely devoid of such enhancements.

The longest and most striking period of relativistic electron scarcity was for much of calendar year 2014. Figure 13 shows this period in some detail. The top panel (Figure 13a) shows the L-sorted, color-coded format used extensively in this paper. The next panel (b) is line "cuts" for daily averaged fluxes of $E = 4.2$-MeV electrons for $L = 3.5$, 4.5, and 5.5 (as indicated by the color of the curves). The lower four panels (c–f) show the solar wind and IMF data we have employed in prior figures.

From Figure 13, one again can understand that the absence of 4.2-MeV electrons for most of the year-long period was directly and rather obviously related to very weak solar wind and IMF drivers. The solar wind speed went above 500 km/s only a few times during the year, as in early January 2014, February, April, and late May. In those cases, only a couple of them had corresponding episodes of southward IMF

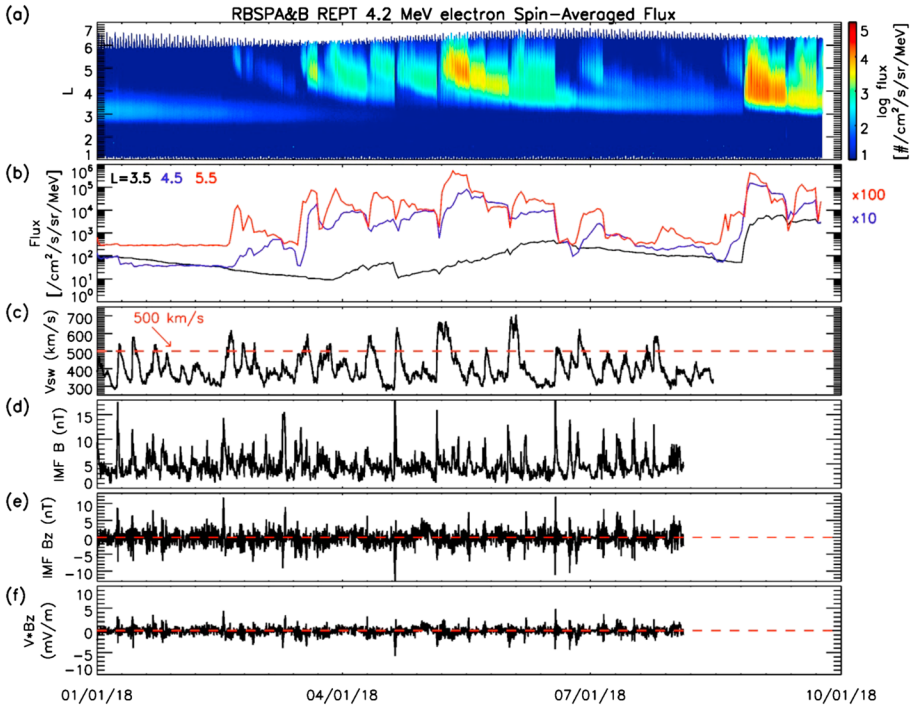

Figure 14. Similar format to Figure 13 but for the time period of 1 January to 1 October 2018. RBSP = Radiation Belt Storm Probes; REPT = Relativistic Electron-Proton Telescope.

(Figure 13e). Hence, it is quite understandable that for most of 2014, the ultrarelativistic electrons were near background levels at all L values because the interplanetary drivers (V_{sw} and B_z) were essentially not sufficient at any time during the year. (There were several solar wind enhancements later in the year from September to December that were geoeffective).

Figure 14 is analogous to Figure 13 but for the period 1 January 2018 to 1 October 2018 (i.e., we have extended a month beyond our 6-year "window"). We see that in January and February 2018 the $L = 4.5$ and $L = 5.5$ fluxes were at background levels. The $L = 3.5$ fluxes were above background but were gradually and systematically decreasing from the activity that had occurred previously in November 2017. There were several solar wind high-speed streams in March through June of 2018. However, none of these had very strong southward IMF. Thus, there were relatively weak, but periodic, flux enhancements in the March–June period. In July and August, the flux values were again near background levels and then the August 2018 solar/geomagnetic activity caused a great resurgence in fluxes at all L values.

8. Discussion and Conclusion

In this paper, we have taken a broad, comprehensive view of high-energy electron measurements from the Van Allen Probes for 6 years of mission lifetime (2012–2018). We have examined key intervals of strong flux enhancements for $1.5 \leq E \leq 12$ MeV using the REPT instrument on board both Van Allen Probes A and B spacecraft. We have also looked closely at extended quiet intervals (as in the year 2014) when multi-MeV electrons were largely absent throughout the entire magnetosphere.

In this extended survey of data, we have confirmed several earlier findings based upon previously more limited data. For example, throughout this 6-year study period, we saw no instance in which multi-MeV electrons penetrated into the inner zone ($L \leq 2.5$) region. This confirms our earlier finding about the seeming "impenetrable barrier" for high-energy electron during the Van Allen Probes era (Baker, Jaynes, Hoxie, et al., 2014; Foster et al., 2016). We fully recognize that high-energy electrons might have breached the barrier had there been stronger solar forcing episodes (Blake et al., 1992; Li et al., 1993, 2005, 2017; Baker, Kanekal, Li, et al., 2004; Zhao & Li, 2013). But, rather remarkably, there have been no such sufficiently strong forcing events throughout Solar Cycle 24 and—as a consequence—the inner Van Allen zone has

had no highly relativistic electrons for at least 6 years. We believe that a deeper theoretical understanding is needed of how ultrarelativistic electrons can be so sharply and persistently excluded rather precisely at $L = 2.8$ even when weeks and months of inward radial diffusion should have been possible (see, for example, Figure 12).

This long-term study has revisited some prior intense acceleration events for high-energy electrons and has also scrutinized some previously unexamined cases. Without exception, we have found that the most prominent strong acceleration events have been associated with solar wind speeds $V_{sw} \geq 500$ km/s. Consistently, Zhao et al. (2018b), through a statistical analysis of the ultrarelativistic electron flux enhancements using over-5-year REPT measurements, showed that the solar wind speed is the most effective solar wind parameter causing the flux enhancements of ultrarelativistic electrons especially for higher energies. Despite this fact having been generally known and appreciated for decades (see Baker et al., 1997, and references therein), we still do not believe that physical models of magnetospheric acceleration adequately explain why such a sharp threshold of radiation belt forcing by the solar wind speed should exist. This thoroughly established observational property should be much better explained as part of the overall solar wind-magnetosphere coupling paradigm.

Finally, as noted above, there have been surprisingly long intervals when multi-MeV electrons were simply not of measurable intensity anywhere within the magnetospheric confines. Obviously, this absence of high-energy electrons is the obverse of the times when electron acceleration events were frequent and strong. Indeed, we have shown here that periods of time with low relativistic electron content in the radiation belts were also times with low solar wind speeds ($V_{sw} < 500$ km/s) and weak IMF B_z components. Since high-energy electrons can—and do—play an important role in atmospheric coupling (Thorne, 1980; Baker et al., 1987), our observations about electron paucity have important implications for middle atmospheric chemistry (e.g., Randall et al., 2015).

In conclusion, we can say that having precise and continuous observations of high-energy electrons throughout the inner magnetosphere for over half a solar cycle has been a propitious circumstance. We believe that from both a scientific perspective and from a practical, that is, space weather, perspective the space physics community should work to assure that such radiation belt measurements within the magnetic equatorial area continue in perpetuity. Only such long-term continuous measurements can assure revelations of all the radiation belts' secrets.

Acknowledgments
The research presented here was supported by RBSP-ECT funding through JHU/APL contract 967399 (under prime NASA contract NAS5-01072). Van Allen Probes REPT data used in this paper are available from the ECT Science Operations and Data Center (http://www.rbsp-ect.lanl.gov). Van Allen Probes Solar wind data and geomagnetic indices are provided by OMNIWeb (http://omniweb.gsfc.nasa.gov/).

References

Baker, D. N., Blake, J. B., Gorney, D. J., Higbie, P. R., Klebesadel, R. W., & King, J. H. (1987). Highly relativistic magnetospheric electrons: A role in coupling to the middle atmosphere. *Geophysical Research Letters*, *14*, 1027–1030.

Baker, D. N., Jaynes, A. N., Hoxie, V. C., Thorne, R. M., Foster, J. C., Li, X., et al. (2014). An impenetrable barrier to ultrarelativistic electrons in the Van Allen radiation belts. *Nature*, *515*(7528), 531–534. https://doi.org/10.1038/nature13956

Baker, D. N., Jaynes, A. N., Kanekal, S. G., Foster, J. C., Erickson, P. J., Fennell, J. F., et al. (2016). Highly relativistic radiation belt electron acceleration, transport, and loss: Large solar storm events of March and June 2015. *Journal of Geophysical Research: Space Physics*, 6647–6660. https://doi.org/10.1002/2016JA022502

Baker, D. N., Jaynes, A. N., Li, X., Henderson, M. G., Kanekal, S. G., Reeves, G. D., et al. (2014). Gradual diffusion and punctuated phase space density enhancements of highly relativistic electrons: Van Allen Probes observations. *Geophysical Research Letters*, *41*, 1351–1358. https://doi.org/10.1002/2013GL058942

Baker, D. N., Kanekal, S. G., & Blake, J. B. (2004). Characterizing the Earth's outer Van Allen zone using a radiation belt content index. *Space Weather*, *2*, S02003. https://doi.org/10.1029/2003SW000026

Baker, D. N., Kanekal, S. G., Hoxie, V. C., Henderson, M. G., Li, X., Spence, H. E., et al. (2013). A long-lived relativistic electron storage ring embedded in Earth's outer Van Allen belt. *Science*, *340*(6129), 186–190. https://doi.org/10.1126/science.1233518

Baker, D. N., Kanekal, S. G., Hoxie, V. C., Batiste, S., Bolton, M., Li, X., et al. (2012). The Relativistic Electron-Proton Telescope (REPT) instrument on board the Radiation Belt Storm Probes (RBSP) spacecraft: Characterization of Earth's radiation belt high-energy particle populations. *Space Science Reviews*, *179*(1-4), 337–381. https://doi.org/10.1007/s11214-012-9950-9

Baker, D. N., Kanekal, S. G., Li, X., Monk, S. P., Goldstein, J., & Burch, J. L. (2004). An extreme distortion of the Van Allen belt arising from the "Halloween" solar storm in 2003. *Nature*, *432*(7019), 878–881. https://doi.org/10.1038/nature03116

Baker, D. N., Li, X., Turner, N., Allen, J. H., Bargatze, L. F., Blake, J. B., et al. (1997). Recurrent geomagnetic storms and relativistic electron enhancements in the outer magnetosphere: ISTP coordinated measurements. *Journal of Geophysical Research*, *102*(A7), 14,141–14,148. https://doi.org/10.1029/97JA00565

Baker, D. N., Reisberg, L., Pankratz, C. K., Panneton, R. S., Giles, B. L., Wilder, F. D., & Ergun, R. E. (2015). Magnetospheric multiscale data acquisition, management and access. *Space Science Research*. https://doi.org/10.1007/s11214-014-0128

Blake, J. B., Kolasinski, W. A., Fillius, R. W., & Mullen, E. G. (1992). Injection of electrons and protons with energies of tens of MeV into L < 3 on 24 March 1991. *Geophysical Research Letters*, *19*(8), 821–824. https://doi.org/10.1029/92GL00624

Foster, J. C., Erickson, P. J., Baker, D. N., Claudepierre, S. G., Kletzing, C. A., Kurth, W., et al. (2014). Prompt energization of relativistic and highly relativistic electrons during a substorm interval: Van Allen Probes observations. *Geophysical Research Letters*, *41*, 20–25. https://doi.org/10.1002/2013GL058438

Foster, J. C., Erickson, P. J., Baker, D. N., Jaynes, A. N., Mishin, E. V., Fennel, J. F., et al. (2016). Observations of the impenetrable barrier, the plasmapause, and the VLF bubble during the 17 March 2015 storm. *Journal of Geophysical Research: Space Physics*, *121*, 5537–5548. https://doi.org/10.1002/2016JA022509

Foster, J. C., Wygant, J. R., Hudson, M. K., Boyd, A. J., Baker, D. N., Erickson, P. J., & Spence, H. E. (2015). Shock-induced prompt relativistic electron acceleration in the inner magnetosphere. *Journal of Geophysical Research: Space Physics*, *120*, 1661–1674. https://doi.org/10.1002/2014JA020642

Jaynes, A. N., Ali, A. F., Elkington, S. R., Malaspina, D. M., Baker, D. N., Li, X., et al. (2018). Fast diffusion of ultra-relativistic electrons in the outer radiation belt: 17 March 2015 storm event. *Geophysical Research Letters*, *45*, 10,874–10,882. https://doi.org/10.1029/2018GL079786

Jaynes, A. N., Lessard, M. R., Takahashi, K., Ali, A. F., Malaspina, D. M., Michell, R. G., et al. (2015). Correlated Pc4–5 ULF waves, whistler-mode chorus, and pulsating aurora observed by the Van Allen Probes and ground-based systems. *Journal of Geophysical Research: Space Physics*, *120*, 8749–8761. https://doi.org/10.1002/2015ja021380

Kanekal, S. G., Baker, D. N., Fennell, J. F., Jones, A., Schiller, Q., Richardson, I. G., et al. (2016). Prompt acceleration of magnetospheric electrons to ultrarelativistic energies by the 17 March 2015 interplanetary shock. *Journal of Geophysical Research: Space Physics*, *121*, 7622–7635. https://doi.org/10.1002/2016JA022506

Kanekal, S. G., Baker, D. N., Henderson, M. G., Li, W., Fennell, J. F., Zheng, Y., et al. (2015). Relativistic electron response to the combined magnetospheric impact of a coronal mass ejection overlapping with a high-speed stream: Van Allen Probes observations. *Journal of Geophysical Research: Space Physics*, *120*, 7629–7641. https://doi.org/10.1002/2015JA021395

Li, X., Baker, D. N., Temerin, M., Reeves, G., Friedel, R., & Shen, C. (2005). Energetic electrons, 50 keV to 6 MeV, at geosynchronous orbit: Their responses to solar wind variations. *Space Weather*, *3*, S04001. https://doi.org/10.1029/2004SW000105

Li, X., Baker, D. N., Zhao, H., Zhang, K., Jaynes, A. N., Schiller, Q., et al. (2017). Radiation belt electron dynamics at low L(<4): Van Allen Probes era versus previous two solar cycles. *Journal of Geophysical Research: Space Physics*, *122*, 5224–5234. https://doi.org/10.1002/2017JA023924

Li, X., Barker, A. B., Baker, D. N., Tu, W. C., Sarris, T. E., Selesnick, R. S., et al. (2009). Modeling the deep penetration of outer belt electrons during the "Halloween" magnetic storm in 2003. *Space Weather*, *7*, S02004. https://doi.org/10.1029/2008SW000418

Li, X., Roth, I., Temerin, M., Wygant, J. R., Hudson, M. K., & Blake, J. B. (1993). Simulation of the prompt energization and transport of radiation belt particles during the March 24, 1991 SSC. *Geophysical Research Letters*, *20*(22), 2423–2426. https://doi.org/10.1029/93GL02701

Li, X., Temerin, M., Baker, D. N., & Reeves, G. D. (2011). Behavior of MeV electrons at geosynchronous orbit during last two solar cycles. *Journal of Geophysical Research*, *116*, A11207. https://doi.org/10.1029/2011JA016934

Mann, I. R., Ozeke, L. G., Murphy, K. R., Claudepierre, S. G., Turner, D. L., Baker, D. N., et al. (2016). Explaining the dynamics of the ultra-relativistic third Van Allen Radiation belt. *Nature Physics*, *12*(10), 978–983. https://doi.org/10.1038/NPHYS3799

McPherron, R. L., Baker, D. N., & Crooker, N. U. (2009). Role of the Russell–McPherron effect in the acceleration of relativistic electrons. *Journal of Atmospheric and Solar-Terrestrial Physics*, *71*(10-11), 1032–1044. https://doi.org/10.1016/j.jastp.2008.11.002

Randall, C. E., Harvey, V. L., Holt, L. A., Marsh, D. R., Kinnison, D., Funke, B., & Bernath, P. F. (2015). Simulation of energetic particle precipitation effects during the 2003–2004 Arctic winter. *Journal of Geophysical Research: Space Physics*, *120*, 5035–5048. https://doi.org/10.1002/2015JA021196

Reeves, G. D., Morley, S. K., Friedel, R. H. W., Henderson, M. G., Cayton, T. E., Cunningham, G., et al. (2011). On the relationship between relativistic electron flux and solar wind velocity: Paulikas and Blake revisited. *Journal of Geophysical Research*, *116*, A02213. https://doi.org/10.1029/2010JA015735

Reeves, G. D., Spence, H. E., Henderson, M. G., Morley, S. K., Friedel, R. H. W., Funsten, H. O., et al. (2013). Electron acceleration in the heart of the Van Allen radiation belts. *Science*, *341*(6149), 991–994. https://doi.org/10.1126/science.1237743

Selesnick, R. S. (2015). Measurement of inner radiation belt electrons with kinetic energy above 1 MeV. *Journal of Geophysical Research: Space Physics*, *120*, 8339–8349. https://doi.org/10.1002/2015JA021387

Selesnick, R. S., Baker, D. N., Kanekal, S. G., Hoxie, V. C., & Li, X. (2018). Modeling the proton radiation belt with Van Allen Probes Relativistic Electron-Proton Telescope data. *Journal of Geophysical Research: Space Physics*, *123*, 685–697. https://doi.org/10.1002/2017JA024661

Shprits, Y. Y., Kellerman, A. C., Drozdov, A. Y., Spence, H. E., Reeves, G. D., & Baker, D. N. (2015). Combined convective and diffusive simulations: VERB-4D comparison with 17 March 2013 Van Allen Probes observations. *Geophysical Research Letters*, *42*, 9600–9608. https://doi.org/10.1002/2015GL065230

Thorne, R. M. (1980). The importance of energetic particle precipitation on the chemical composition of the middle atmosphere. *Pure and Applied Geophysics*, *118*, 128–151.

Thorne, R. M., Li, W., Ni, B., Ma, Q., Bortnik, J., Chen, L., et al. (2013). Rapid local acceleration of relativistic radiation-belt electrons by magnetospheric chorus. *Nature*, *504*(7480), 411–414. https://doi.org/10.1038/nature12889

Xiang, Z., Tu, W., Li, X., Ni, B., Morley, S. K., & Baker, D. N. (2017). Understanding the mechanisms of radiation belt dropouts observed by Van Allen Probes. *Journal of Geophysical Research: Space Physics*, *122*, 9858–9879. https://doi.org/10.1002/2017JA024487

Zhao, H., Baker, D. N., Jaynes, A. N., Li, X., Elkington, S. R., Kanekal, S. G., et al. (2017). On the relation between radiation belt electrons and solar wind parameters/geomagnetic indices: Dependence on the first adiabatic invariant and L*. *Journal of Geophysical Research: Space Physics*, *122*, 1624–1642. https://doi.org/10.1002/2016JA023658

Zhao, H., Baker, D. N., Li, X., Jaynes, A. N., & Kanekal, S. G. (2018a). The acceleration of ultrarelativistic electrons during a small to moderate storm of 21 April 2017. *Geophysical Research Letters*, *45*, 5818–5825. https://doi.org/10.1029/2018GL078582

Zhao, H., Baker, D. N., Li, X., Jaynes, A. N., & Kanekal, S. G. (2018b). The effects of geomagnetic storms and solar wind conditions on the ultrarelativistic electron flux enhancements. *Journal of Geophysical Research: Space Physics*, *124*. https://doi.org/10.1029/2018JA026257

Zhao, H., & Li, X. (2013). Inward shift of outer radiation belt electrons as a function of Dst index and the influence of the solar wind on electron injections into the slot region. *Journal of Geophysical Research: Space Physics*, *118*, 756–764. https://doi.org/10.1029/2012JA018179